Electronic Supplementary Information I for:

Superelastic metal microsprings as fluidic sensors and actuators

Weiming Li,[a‡] *Gaoshan Huang,*[a,‡,*] *Jiao Wang,*[a] *Ying Yu,*[a] *Xiaojing Wu,*[a,*] *Xugao Cui,*[b] *and Yongfeng Mei*[a,c*]

[a] Department of Materials Science, Fudan University, Shanghai 200433, China y. E-mail: gshuang@fudan.edu.cn, wuxj@fudan.edu.cn, and yfm@fudan.edu.cn

[b] Department of Light Sources & Illuminating Engineering, School of Information Science & Engineering, Fudan University, Shanghai 200433, China.

[c] Key Disciplines Lab of Novel Micro-nano Device and systems Technology & Microsystem Research Center, Chongqing University, Chongqing 400044, China.

[‡]These authors contributed equally to this work.

[*] Email: gshuang@fudan.edu.cn, wuxj@fudan.edu.cn, and yfm@fudan.edu.cn

1. Geometry of obtained Ti microsprings.

Table S1. Geometric parameters of typical microsprings investigated in the experiments.

R_0 (μm)	p_0 (μm)	Helicity angle θ_0 (deg)	Misaligned angle α (deg)
13	31.8	21.3	20
14.4	64.8	35.6	35
9.4	49.5	40.0	40
8.8	54.6	44.7	45
9.7	78.9	52.4	50
7.1	84.2	62.1	60
8.8	189.7	73.8	75

2. Controllable fabrication of microsprings.

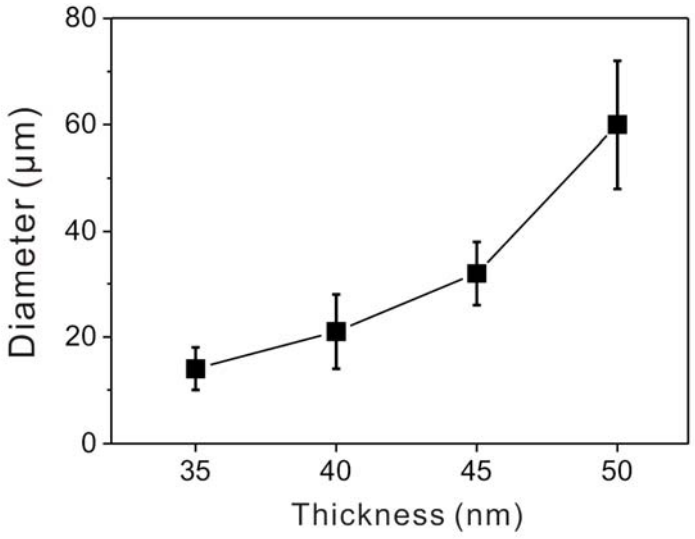

Figure S1. The diameter of Ti microspring as a function of the thickness of Ti nanomembrane.

Figure S1 shows the relationship between the diameters of Ti microsprings and thicknesses of Ti nanomembranes. It can be observed that the diameter increases obviously with the increasing nanomembrane thickness, suggesting a good way in diameter tuning.

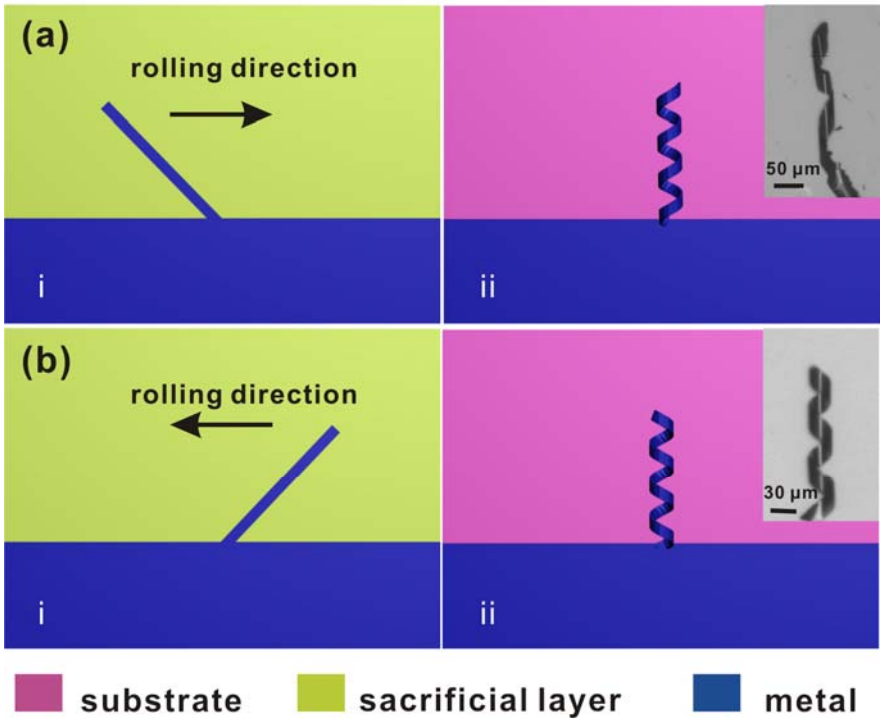

Figure S2. Schematic diagrams illustrating the method to control the chirality of microsprings: (a) the right-handed microspring and (b) the left-handed microspring. The corresponding insets show optical microscope images of the fabricated Ti microsprings.

Figure S2 schematically diagrams illustrates the method to control the chiralities of the microsprings by altering the orientations of metal strips. In our experiment, the metal strips roll up rather than roll down. Thus, the right-handed microspring can be obtained when the strip's orientation is designed as in Figure S2(a), while left-handed microsprings are fabricated if the strip is oriented as in Figure S2(b). In one word, the chirality of the microspring is controllable by patterning metal strip with different α. The optical microscope images of microsprings with different chiralities showing in the corresponding insets prove the feasibility of this method.

3. Mathematical derivation of *v*-*x* relationship.

Equation (1) is derived from the balance of forces:

$$\frac{x}{v} = \frac{12\mu n^2 p^2 R}{G(1+\upsilon_{Poisson})\left[\ln\left(\frac{2L}{R}\right) - 0.72\right]t^3}, \tag{S1}$$

which can be written as

$$v = \frac{G(1+\upsilon_{Poisson})t^3}{12\mu} \bullet \frac{\left[\ln\left(\frac{2L}{R}\right) - 0.72\right]}{n^2 p^2 R} \bullet x. \tag{S2}$$

Assuming that n is a constant during the deformation, we can obtain the geometric constraint:

$$L = np_0 + x, \tag{S3}$$

$$np = np_0 + x, \tag{S4}$$

$$4\pi^2 R^2 + p^2 = 4\pi^2 R_0^2 + p_0^2 \tag{S5}$$

Combining equations (2), (3), (4), and (5), we thus get the relation between v and x as

$$v = \frac{\pi G(1+\upsilon_{Poisson})t^3}{6\mu} \bullet \frac{\ln\left[\frac{4\pi(np_0+x)}{\sqrt{4\pi^2 R_0^2 + p_0^2 - \frac{(np_0+x)^2}{n^2}}}\right] - 0.72}{(np_0+x)^2\sqrt{4\pi^2 R_0^2 + p_0^2 - \frac{(np_0+x)^2}{n^2}}} \bullet x. \tag{S6}$$

The values of R_0, p_0, and n are obtained from optical microscopy, as listed in Table S2.

Table S2. Geometric parameters of Ti microsprings in relaxed states.

	R_0 (μm)	p_0 (μm)	n
SP1	9.4	90	2
SP2	9.8	61	3.5
SP3	9.6	54	4.8

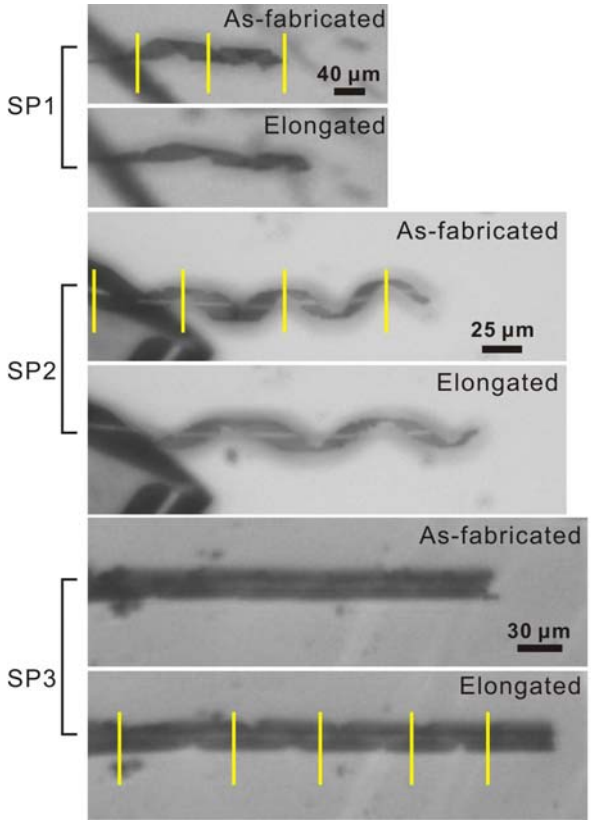

Figure S3. Optical images of Ti microsprings SP1, SP2, and SP3.

4. Influence of microspring geometry on *v*-*x* relationship.

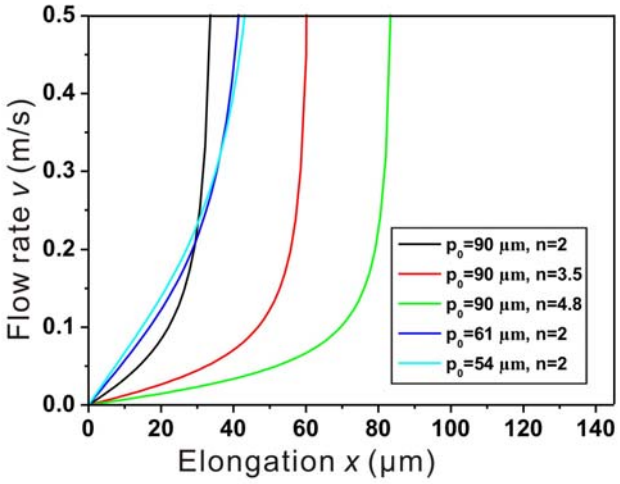

Figure S4. *v*-*x* curves derived from equation (6), with R_0=9.4 μm.

To further identify the influence of microspring geometry on the mechanical properties, we calculated the v as a function of x using equation (S6) and the results are plotted in Figure S2. For the microsprings with n=2, we found that the elongations change little as p_0 decreases from 90 to 54 μm. However, a noticeable change is observed when n increases from 2 to 4.8, while p_0 is kept at 90 μm. Hence, it can be inferred that n dominates the elongation of the microspring in flowing water while p_0 has relatively little effect.